



Iranian Research Organization
for Science and Technology
(IROST)

$\text{Fe}_3\text{O}_4@\text{SiO}_2/\text{AEPTMS}/\text{Fe}(\text{OTf})_3$: An efficient superparamagnetic nanocatalyst for the protecting of alcohols

Somayeh Mehdigholami^{1,✉}, Esmail Koohestanian²

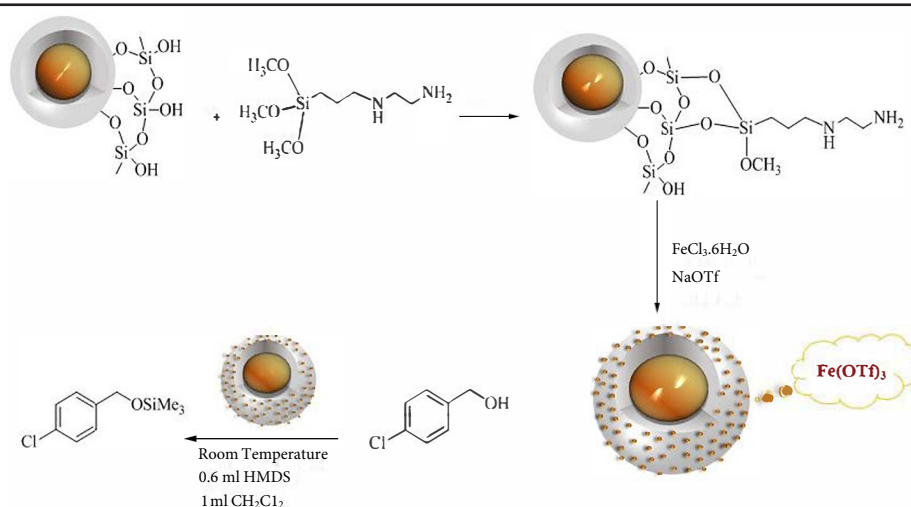
¹ Institute of Nanoscience and Nanotechnology, University of Kashan, Kashan, Iran

² Department of Chemical Engineering, Islamic Azad University, Iranshahr Branch, Iranshahr, Iran

HIGHLIGHTS

- Synthesis of $\text{Fe}_3\text{O}_4@\text{SiO}_2/\text{AEPTMS}/\text{Fe}(\text{OTf})_3$ as magnetic nanocatalyst.
- Synthesis of fine spherical nanoparticles without agglomeration.
- These nanocatalysts were used to protect the hydroxyl group in aromatic and linear alcohols.

GRAPHICAL ABSTRACT



ARTICLE INFO

Article type:

Research article

Article history:

Received 21 March 2023

Revised 26 May 2023

Accepted 28 May 2023

Keywords:

Hydroxy compounds

Magnetic iron oxide

Nanoparticles

Catalytic activity

DOI: [10.22104/JPST.2023.6188.1224](https://doi.org/10.22104/JPST.2023.6188.1224)

ABSTRACT

$\text{Fe}_3\text{O}_4@\text{SiO}_2/\text{AEPTMS}/\text{Fe}(\text{OTf})_3$ is a stable, effective, and magnetic nanocatalyst easily prepared and characterized using FT-IR spectroscopy, SEM, TEM, and VSM techniques. This nanocatalyst was successfully applied for trimethylsilylation of numerous alcohols (primary, secondary, and tertiary alcohols) with hexamethyldisilazane in 1 ml dichloromethane at room temperature to their corresponding trimethylsilyl (TMS) ethers. Quick response times and a simple reprocessing procedure are two fascinating advantages of this nanocatalyst. This catalyst protects alcohols at 1.5 min, and turn-over frequency (TOF) values for the presented catalytic system have been estimated 833 h^{-1} .



© The Author(s).

Published by IROST.

1. Introduction

Protecting hydroxy compounds is a necessary step for numerous chemical processes, including synthesizing pharmaceuticals and organic materials [1]. Various industrial catalysts facilitate these processes. Such catalysts include TiO_2 [2], $\text{Fe}_3\text{O}_4@\text{CeO}_2/\text{SO}_4^{2-}$ [3], Zn complex supported on magnetic nanoparticles [4], InBr_3 [5], ZrCl_4 [6], and molybdophosphovanadates supported on commercial alumina [7]. Several studies have been conducted to describe the reaction conditions in the presence of a catalyst. For example, Ghafari *et al.* presented the $\text{Fe}_3\text{O}_4@\text{ZrO}_2/\text{SO}_4^{2-}$ catalyst to protect alcohol using a mixture of alcohol (1.0 mmol) and HMDS (1.5 mmol) within the catalyst (80 mg) for this process, which resulted in a reaction time of 15 min with 90 % yield [8]. Zolfigol *et al.* investigated 1 mmol nano-MCM-41@ $(\text{CH}_2)_3$ -1-methylimidazole] Br_3 to protect the alcohol using a mixture of alcohol or phenol (1 mmol) and HMDS (2 mmol) in CH_2Cl_2 (5 ml) [9]. The time of this reaction was 35 min with a 96 % yield. Zareyee and coworkers used the CMK-5- SO_3H catalyst for TMS – alcohol in 3 ml CH_2Cl_2 in 30 min with a 90 % yield [10]. Abri *et al.* expended (0.03 mol) $\text{NaHSO}_4.\text{SiO}_2$ (nano) for the TMS-alcohol at room temperature in 7 min in free solvents [11]. Table 1 compares the activity of different catalysts to protect alcohols with HMDS showing that retrievability and reutilization of catalysts are vital for a variety of catalytic processes.

Magnetic nanoparticles, which are superparamagnetic materials, can be easily separated with an external magnet without filtration, centrifugation periods, or complex workups [12,13]. Thus, restricting catalyst onto magnetic nanoparticles boosts high surface area-to-volume ratios that enhance catalyst accessibility and activity. Magnetic nanoparticles have been produced applying a variety of substances and techniques [14-16], such as co-precipitation [15], micro emulsion [16], thermal decomposition [17], and hydrothermal synthesis [18]. Of these, a co-precipitation is a practical approach for producing magnetic nanoparticles from an iron salt mixture in the presence of a base; this process is associated with high yields and comparatively narrow size distributions [19]. The oxidation and deformation of the magnetization properties of magnetic nanoparticles can be improved by covering them with polymers or other agents [20]. Silica is frequently used for veneering the surface of MNPs [21] due to its capacity to completely stabilize the magnetic nano core as well as provide greater possibilities for surface alteration through its terminally-functionalized silanol groups [22-25]. These groups can interact with various coupling agents to covalently attach particular ligands to the surfaces of

Table 1. A comparison of the efficiency of $\text{Fe}_3\text{O}_4@\text{SiO}_2/\text{AEPTMS}/\text{Fe}(\text{OTf})_3$ with other catalysts for silylation of 4-chlorobenzyl alcohol using HMDS at room temperature.

Entry	Catalyst	Solvent	Time (min)	Yield (%)	Ref.
1	$\text{Fe}_3\text{O}_4@\text{ZrO}_2/\text{SO}_4^{2-}$	free	15	90	[8]
2	Nano-MCM-41@ $(\text{CH}_2)_3$ -1-methylimidazole] Br_3	CH_2Cl_2	35	96	[9]
3	CMK-5- SO_3H	CH_2Cl_2	30	99	[10]
4	$\text{NaHSO}_4.\text{SiO}_2$ (nano)	CH_3CN	7	90	[11]
5	$\text{Fe}_3\text{O}_4@\text{CeO}_2/\text{SO}_4^{2-}$	free	15	93	[3]
6	This work	CH_2Cl_2	1.5	100	

these magnetic nanoparticles [26], with N-(2-aminoethyl)-3-aminopropyl-trimethoxysilane being an appropriate modifier for silica NPs. This compound has methoxysilane ($\text{Si}-\text{OCH}_3$) functioning as the anchoring group and the amino ($-\text{NH}_2$) faction as the charging group [27].

To better conserve the environment, it is necessary to substitute toxic and expensive metal catalysts for inexpensive, easily obtainable, and non-toxic alternatives. Iron has been extensively studied as a prospective replacement catalyst for various organic reactions due to its abundance, low cost, non-toxicity, and eco-friendly characteristics [28]. A multitude of iron-catalyzed oxidations [31,32] hydrogenations [28,29], rearrangements [33,34], and epoxidations [35,36] have been identified and successfully implemented.

In this study, we have prepared a new nanocomposite of Fe_3O_4 (as the magnetic core) and SiO_2 (as the shell) containing AEPTMS functionalities that can be employed as a promising new recyclable catalyst for reactions needing acidic catalysts to speed up. After identification of the prepared catalyst ($\text{Fe}_3\text{O}_4@\text{SiO}_2/\text{AEPTMS}/\text{Fe}(\text{OTf})_3$), its ability to protect aromatic and aliphatic alcohols was tested.

2. Experimental

General chemicals were obtained from Merck and Aldrich Chemical Companies. Yields reported refer to the isolated pure products. Water used in all experiments was purified by a Milli-Q plus 185 water purification system (Millipore, Bedford, MA, USA). The products were characterized by comparing their spectral diffuse-reflectance and FT-IR spectra obtained as potassium bromide pellets within the range 400 - 4000 cm^{-1} with a JASCO 6300 spectrophotometer. Experiments were performed using a Shimadzu GC-16A instrument in $\text{Fe}_3\text{O}_4@\text{SiO}_2\text{-CAA}$ with a 2 m column packed

with silicon DC-200 or Carbowax 20 m. Transmission electron micrographs of magnetic nanoparticles were documented on a Philips CM 120 TEM instrument. Samples were sent to the Meghnatis Daghigh Kavir Co. for magnetic measurement using a vibrating sample magnetometer (VSM). The ultrasonic equipment used to synthesize MNPs was a Bandelin electronic ultrasonic bath DT 514 BH-RC 3095, with a working frequency of 40 kHz.

2.1. Preparation of $Fe_3O_4@SiO_2/AEAPTMS$ nanoparticles

The preparation of Magnetite (Fe_3O_4) particles was carried out via the co-precipitation method. In this method, $FeCl_3 \cdot 6H_2O$ (8.5 g, 31.45 mmol) and $FeCl_2 \cdot 4H_2O$ (3.0 g, 15.27 mmol) were dissolved in 38 ml of 0.4 M HCl solution under an argon atmosphere. The resulting black precipitate formed within 375 ml of a 28 wt % aqueous NH_4OH solution. After which, it was subjected to vigorous stirring at room temperature for 30 min. The black precipitate was collected with an external magnet beneath the reaction flask while the supernatant was decanted and washed with deionized water three times. Finally, the sediment was redispersed in 150 ml of deionized water. Next, 50 ml of this suspension along with 20 ml of 2-propanol were stirred in an ultrasound bath for 20 min before adding 11.58 ml PEG-400, 25 ml of 28 % ammonium hydroxide, 50 ml of deionized water, and 30 ml of tetraethoxysilane (TEOS). Then, N-(2-aminoethyl)-3-aminopropyltrimethoxysilane (AEAPTMS), as a modifier,

was blended into the suspension and stirred for 24 h in an argon gas atmosphere. The resulting black precipitate was collected using a permanent magnet and washed with water and ethanol three times. The product was then dried under a vacuum. The nitrogen content was determined to be 1.3 % by elemental analysis.

2.2. Synthesis of $Fe(OTf)_3$ immobilized on functionalized MNPs

To immobilize $FeCl_3$ on the amino-functionalized magnetite nanoparticles, 300 mg of $FeCl_3$ and 500 mg of the precipitate from the previous step ($Fe_3O_4@SiO_2/AEAPTMS$) were refluxed in acetonitrile for 48 h. The precipitate was collected with an external magnet and washed with ethanol three times before being dried under a vacuum. In the final step, the chlorine ligand was substituted with OTF-via a reaction of the resulting solid with NaOTf in tetrahydrofuran (Fig. 1).

2.3. Typical trimethylsilylation procedure of alcohols and phenols

The reaction of 1 mmol of alcohol or phenol, 1 ml of CH_2Cl_2 , 0.048 mmol of catalyst, and 0.6 mmol per OH group of HMDS was conducted for 1.5 min with vigorous stirring at room temperature. The progress of the reaction was evaluated by gas chromatography (GC).

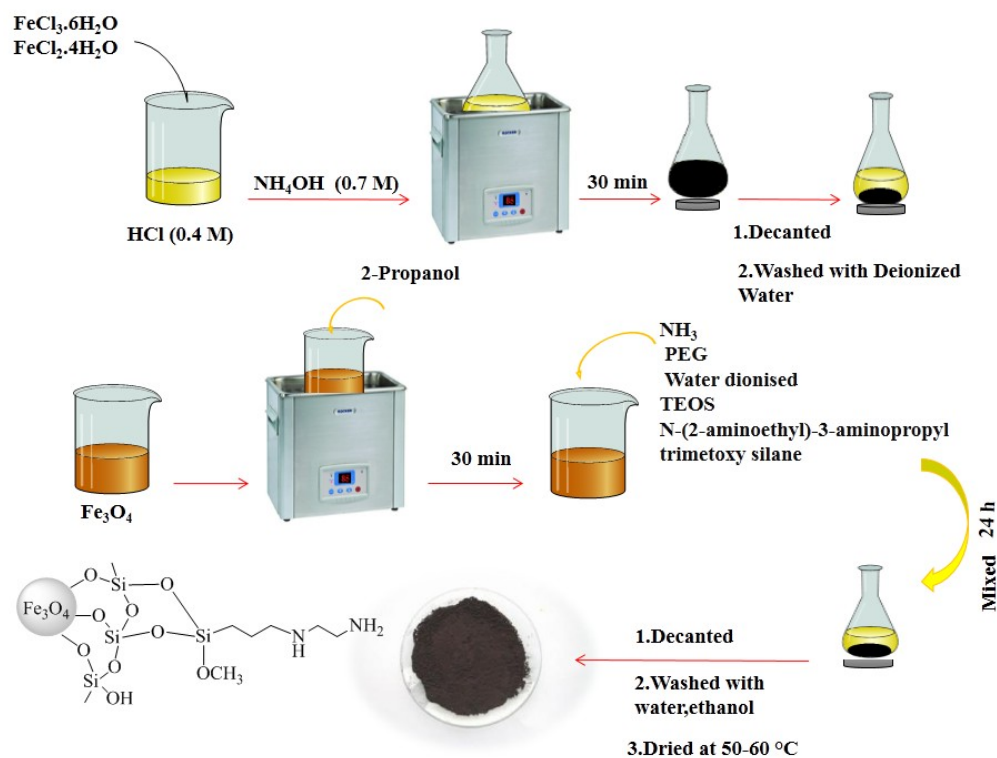


Fig. 1. Scheme of synthesis procedure of $Fe_3O_4@SiO_2/AEAPTMS/Fe(OTf)_3$ nanoparticles.

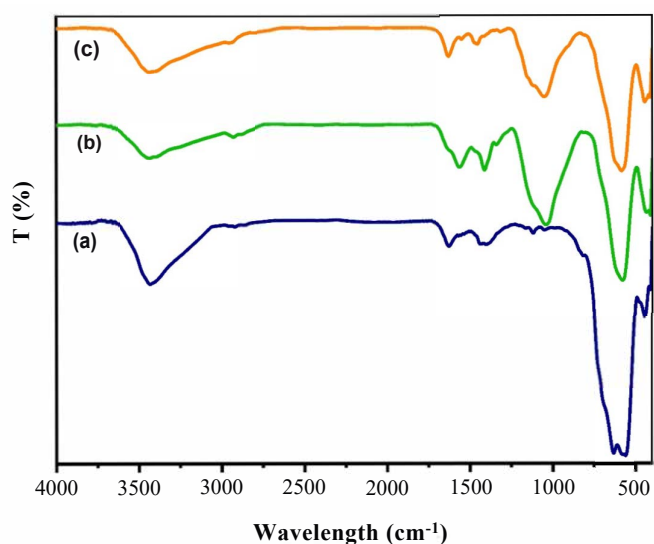


Fig. 2. FT-IR spectrum related to (a) Fe_3O_4 , (b) $\text{Fe}_3\text{O}_4@SiO_2/AEAPTMS$, and (c) $\text{Fe}_3\text{O}_4@SiO_2/AEAPTMS/Fe(OTf)_3$.

3. Results and discussion

3.1. Analysis of the characteristics of immobilized $\text{Fe}_3\text{O}_4@SiO_2/AEAPTMS/Fe(OTf)_3$ nanocatalyst

$\text{Fe}_3\text{O}_4@SiO_2/AEAPTMS/Fe(OTf)_3$, a novel heterogeneous nanocatalyst, was studied and characterized by Fourier transform-infrared (FT-IR), scanning electron microscopy (SEM), transmission electron microscopy (TEM), vibrating-sample magnetometry (VSM) analysis of the saturation magnetization, and energy dispersive X-ray (EDX) for elemental analysis of nanoparticles. FT-IR analysis characterized the functional group variation (Fig. 2), demonstrating the expected Fe–O stretching absorption at 590.1 cm^{-1} (Fig. 2(a)). The peaks for all samples at 3434 , 1038 , and 590 cm^{-1} were attributed to O–H, Si–O, and Fe–O, respectively. Fe_3O_4 anchored on silica-coated nanoparticles showed the expected principal bands [37]. The C–H deformation band was visible at 1406 cm^{-1} , and a sharp band at 1559.2 cm^{-1} was assigned to the C–N stretching vibration of the amine group of AEAPTMS. Furthermore, the peaks at 2848 and 2959 cm^{-1} were attributed to the propyl group [38].

The morphology of the catalyst's surface was observed by SEM micrographs, which showed most of the particles were quasi-spherical in shape (Fig. 3). A histogram related to the SEM image of $\text{Fe}_3\text{O}_4@SiO_2/AEAPTMS/Fe(OTf)_3$ catalyst nanoparticles showed that particles ranged in size from 10 - 80 nm , with most of the particle sizes about 40 - 50 nm .

Fig. 4 depicts the TEM images of these nanoparticles, demonstrating their homogeneous dispersal. The average MNPs particle size was determined to be approximately 40 - 50 nm , without any agglomeration. Subsequent magnification of the TEM image revealed that the MNPs

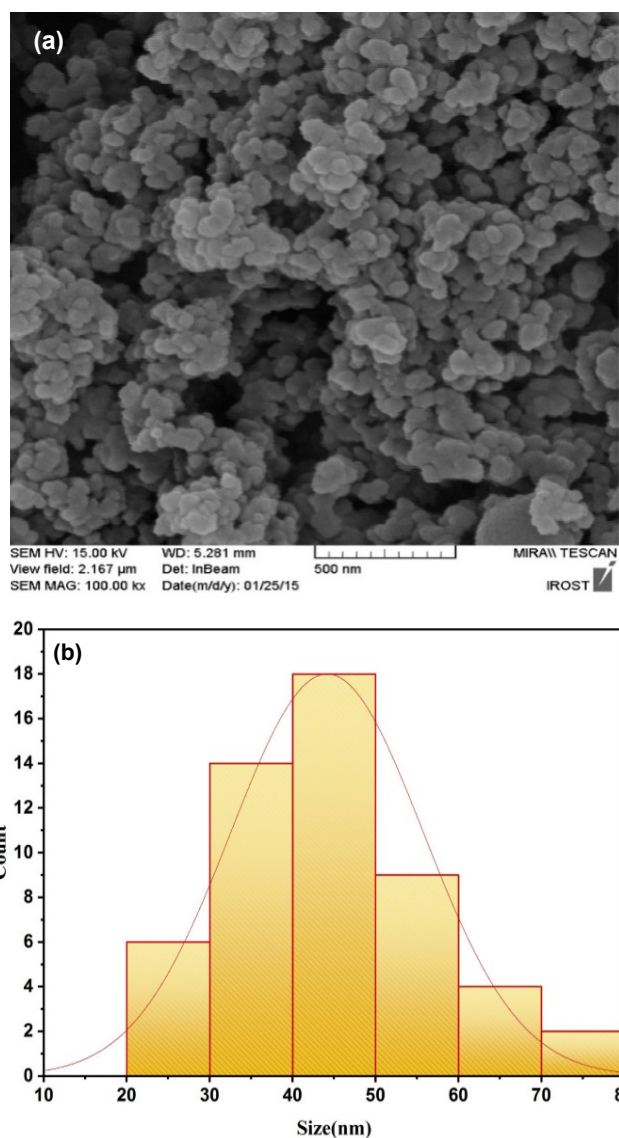


Fig. 3. (a) SEM electron microscope image of $\text{Fe}_3\text{O}_4@SiO_2/AEAPTMS/Fe(OTf)_3$ catalyst nanoparticles. (b) Histogram related to the SEM electron microscope image of $\text{Fe}_3\text{O}_4@SiO_2/AEAPTMS/Fe(OTf)_3$ catalyst nanoparticles.

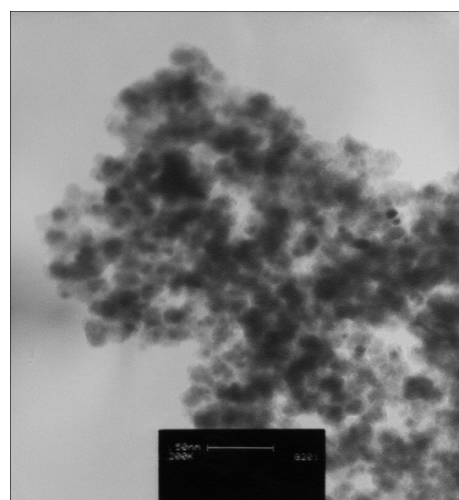


Fig. 4. TEM electron microscope image of $\text{Fe}_3\text{O}_4@SiO_2/AEAPTMS/Fe(OTf)_3$ nanoparticles on a scale of 50 nm .

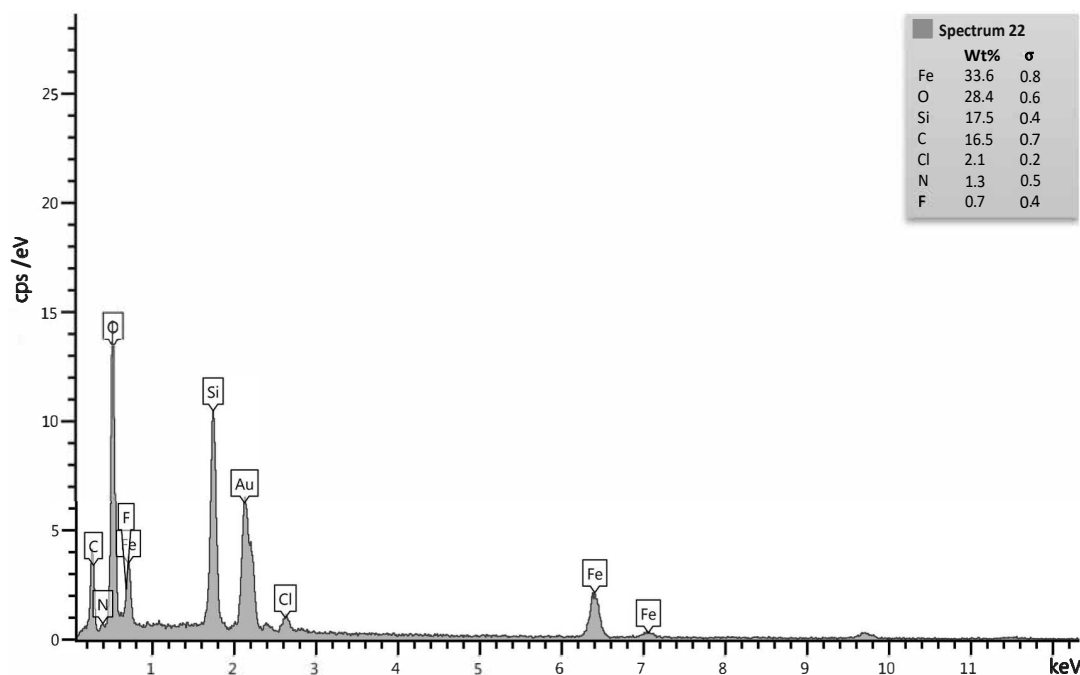


Fig. 5. The results of EDAX analysis of $\text{Fe}_3\text{O}_4@/\text{SiO}_2/\text{AEPTMS}/\text{Fe}(\text{OTf})_3$ catalyst nanoparticles.

possess a spherical shape, corroborating the SEM results.

Energy dispersive X-ray analysis gives an elemental analysis of nanoparticles. The EDAX spectrum of $\text{Fe}_3\text{O}_4@/\text{SiO}_2/\text{AEPTMS}/\text{Fe}(\text{OTf})_3$ MNPs is illustrated in Fig. 5. The EDAX data for $\text{Fe}_3\text{O}_4@/\text{SiO}_2/\text{AEPTMS}/\text{Fe}(\text{OTf})_3$ showed the weight percentage of Fe 33.6 %, O 28.4 %, Si 17.5 %, N 1.3 %, C 16.5 %, and F 0.7 %.

One crucial factor is the high saturation magnetization, which quantifies the maximum magnetic strength. Based on the provided graphs, VSM analysis of $\text{Fe}_3\text{O}_4@/\text{SiO}_2/\text{AEPTMS}/\text{Fe}(\text{OTf})_3$'s magnetization curve showed that the saturation magnetization values for Fe_3O_4 , $\text{Fe}_3\text{O}_4@/\text{SiO}_2$, and $\text{Fe}_3\text{O}_4@/\text{SiO}_2/\text{AEPTMS}/\text{Fe}(\text{OTf})_3$ nanoparticles were 65.57, 41.30, and 37.39 $\text{emu}\cdot\text{g}^{-1}$, respectively. Despite the silica coating (as a non-magnetic material) reducing the saturation magnetization, the nanoparticles still exhibited sufficient levels of magnetism for magnetic separation using an ordinary magnet. As shown in Fig. 6, there is no hysteresis loop in the magnetization curve, proving that the synthesized $\text{Fe}_3\text{O}_4@/\text{SiO}_2/\text{AEPTMS}/\text{Fe}(\text{OTf})_3$ catalyst nanoparticles are superparamagnetic and can be easily separated from the mixture with an external magnetite field (Fig. 6) [39].

3.2. Catalytic performance of $\text{Fe}_3\text{O}_4@/\text{SiO}_2/\text{AEPTMS}/\text{Fe}(\text{OTf})_3$ nanoparticles

The catalytic performance was assessed by utilization of turnover frequency (TOF) values, denoted as $(\text{TOF}) = \text{TON}/\text{time}$ of the reaction. The turnover number (TON) is represented by the number of moles of reactant consumed

per mole of catalyst. TOF determinations were executed utilizing Eqs. (1) and (2) [40].

$$\text{TON} = \text{mole product obtained} / \text{mole catalyst} \quad (1)$$

$$\text{TOF} (\text{h}^{-1}) = \text{TON} / \text{reaction time (h)} \quad (2)$$

The TOF of the catalyst is reported in Table 2. A proposed mechanism for these reactions is shown in Fig. 7. The strategy of this mechanism is a Lewis acid-base interaction, i.e., when the nitrogen atom of hexamethyldisilazane (which has a basic property) is linked to iron (Lewin acid), an active intermediate is formed (1). When the oxygen group

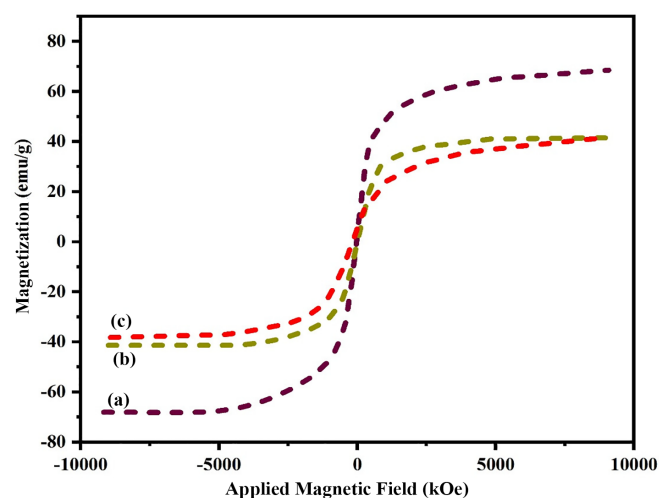
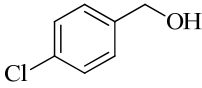
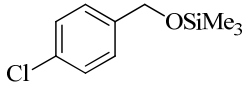
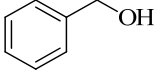
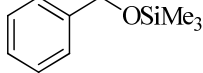
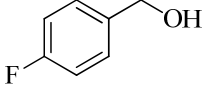
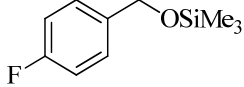
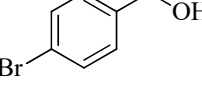
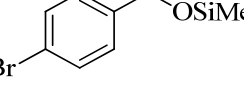
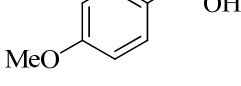
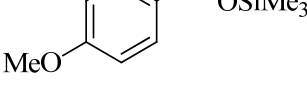
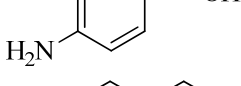
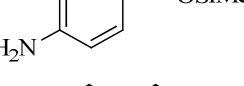
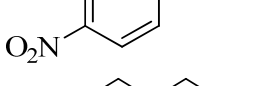
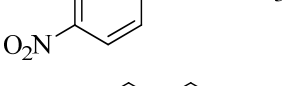
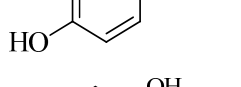
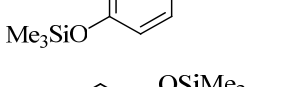
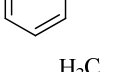
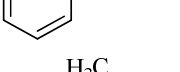
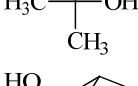
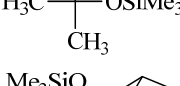
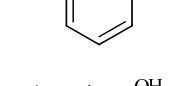
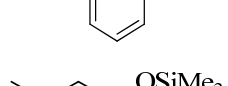
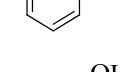
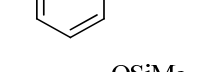
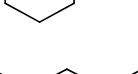
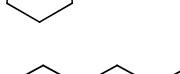
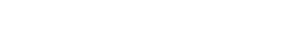


Fig. 6. VSM diagrams of (a) Fe_3O_4 , (b) $\text{Fe}_3\text{O}_4@/\text{SiO}_2$, and (c) $\text{Fe}_3\text{O}_4@/\text{SiO}_2/\text{AEPTMS}/\text{Fe}(\text{OTf})_3$.

Table 2. Trimethylsilylation of alcohols and phenols with HMDS catalyzed by $\text{Fe}_3\text{O}_4@\text{SiO}_2/\text{AEPTMS}/\text{Fe}(\text{OTf})_3$ at room temperature.^a

Entry	Hydroxy compound	TMS-ether	Time (min)	Yield ^c (%)	TOF (h^{-1})
1			1.5	100	833
2			1.5	100	833
3			1.5	100	833
4			1.5	100	833
5			1.5	100	833
6			1.5	100	833
7			1.5	100	833
8 ^b			3	93	378
9			2	97	808
10			2	96	600
11			3	95	395
12 ^b			3	93	387
13			3	100	416
14			3	93	387
15			3	95	395

^a Reaction conditions: Alcohol or phenol (1 mmol), HMDS (0.6 mmol), catalyst (20 mg, 0.04 mmol Fe), CH_2Cl_2 (1 ml).^b Reaction was performed with 0.6 mmol of HMDS per OH group.^c GC yield.

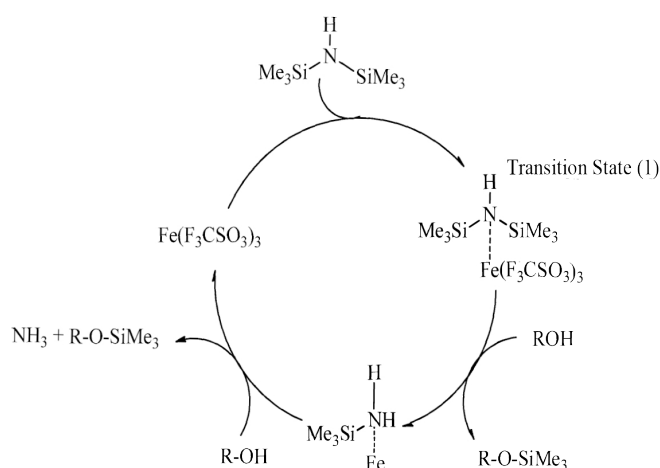


Fig. 7. Proposed mechanism for trimethylsilylation of alcohols and phenols with $\text{Fe}_3\text{O}_4@\text{SiO}_2/\text{AEPTMS}/\text{Fe}(\text{OTf})_3$.

attacks this intermediate, silyl ether compounds are formed, and the catalyst is released for the next cycle. The release of ammonia gas, which can be detected with litmus paper, confirms this mechanism.

3.3. Catalyst recycling

The reusability of the catalyst was assessed by utilizing 4-chlorobenzyl alcohol as a model substrate. Catalyst recycling experiments were conducted using an external magnet, after which the solution was removed with a pipette, and the solid was washed twice with 1,2-dichloroethane. A fresh substrate dissolved in the same solvent was then added to the flask and allowed to proceed for the next run. The catalyst was consecutively reused seven times without any noticeable decline in its catalytic activity.

4. Conclusions

In summary, facile, effective, and environmentally-friendly techniques have been developed for the trimethylsilylation of primary and secondary alcohols in the presence of a high-performing $\text{Fe}_3\text{O}_4@\text{SiO}_2/\text{AEPTMS}/\text{Fe}(\text{OTf})_3$ catalyst. These methods utilize readily-available, cost-effective, and stable reagents while offering operational simplicity, practicality, and yields ranging from good to high. Magnetic separation could be easily used to separate and recycle the catalyst, with the catalyst exhibiting a high degree of reusability with only minimal loss of activity over seven cycles.

This catalyst exhibits several benefits when employed in the specified reactions. Firstly, it can be readily extracted from the mixture via external magnetic manipulation, facilitating recovery and reuse. Secondly, the reactions proceed with notable effectiveness and rapidity. Thirdly, the absence of this catalyst severely impedes progress in these reactions.

Lastly, only a small quantity of this catalyst is required to reactions with high yields in several minutes.

Disclosure statement

No potential conflict of interest was reported by the authors.

References

- [1] Wuts, P. G. M., & Greene, T. W. (2006). *Greene's Protective Groups in Organic Synthesis*. John Wiley & Sons.
- [2] Azad, A., Dekamin, M. G., Afshar, S., Tadjarodi, A., & Mollahosseini, A. (2018). Activation of hexamethyldisilazane (HMDS) by TiO_2 nanoparticles for protection of alcohols and phenols: The effect of the catalyst phase on catalytic activity. *Research on Chemical Intermediates*, 44, 2951-2963. <https://doi.org/10.1007/s11164-016-2519-6>
- [3] Mohammadiyan, E., Ghafuri, H., & Kakanejadifard, A. (2019). Synthesis and characterization of a bifunctional nanomagnetic solid acid catalyst ($\text{Fe}_3\text{O}_4@\text{CeO}_2/\text{SO}_4^{2-}$) and investigation of its efficiency in the protection process of alcohols and phenols via hexamethyldisilazane under solvent-free conditions. *Journal of the Chinese Chemical Society*, 66(2), 171-178. <https://doi.org/10.1002/jccs.201800056>
- [4] Uozumi, Y., & Tazawa, A. (2021). Protection and deprotection of alcohols by using a Zn complex supported on magnetic nanoparticles. *Synfacts*, 17(7), 801. <https://doi.org/10.1055/s-0040-1720418>
- [5] Sridhar, M., Raveendra, J., Ramanaiyah, B. C., & Narsaiah, C. (2011). An efficient synthesis of silyl ethers of primary alcohols, secondary alcohols, phenols and oximes with a hydrosilane using InBr_3 as a catalyst. *Tetrahedron Letters*, 52(45), 5980-5982. <https://doi.org/10.1016/j.tetlet.2011.08.151>
- [6] Shirini, F., & Mollarazi, E. (2007). Efficient trimethylsilylation of alcohols and phenols in the presence of ZrCl_4 as a reusable catalyst. *Catalysis Communications*, 8(9), 1393-1396. <https://doi.org/10.1016/j.catcom.2006.11.015>
- [7] Villabrille, P., Romanelli, G., Quaranta, N., & Vázquez, P. (2010). An efficient catalytic route for the preparation of silyl ethers using alumina-supported heteropolyoxometalates. *Applied Catalysis B: Environmental*, 96(3), 379-386. <https://doi.org/10.1016/j.apcatb.2010.02.035>
- [8] Ghafuri, H., Paravand, F., & Rashidizadeh, A. (2017). Nano $\text{Fe}_3\text{O}_4@\text{ZrO}_2/\text{SO}_4^{2-}$: A highly efficient catalyst for the protection and deprotection of hydroxyl groups using HMDS under solvent-free condition. *Phosphorus, Sulfur, and Silicon and the Related Elements*, 192(1), 129-135. <https://doi.org/10.1080/10426507.2016.1236104>

- [9] Zolfigol, M. A., Sajjadifar, S., Ghorbani-Choghamarani, A., & Tami, F. (2018). Application of a novel nano-immobilization of ionic liquid on an MCM-41 system for trimethylsilylation of alcohols and phenols with hexamethyldisilazane. *Research on Chemical Intermediates*, 44, 7093-7106. <https://doi.org/10.1007/s11164-018-3544-4>
- [10] Zareyee, D., Ghandali, M. S., & Khalilzadeh, M. A. (2011). Sulfonated ordered nanoporous carbon (CMK-5-SO₃H) as an efficient and highly recyclable catalyst for the silylation of alcohols and phenols with hexamethyldisilazane (HMDS). *Catalysis Letters*, 141, 1521-1525. <https://doi.org/10.1007/s10562-011-0621-3>
- [11] Abri, A., & Ranjdar, S. (2014). Preparation of nano silica supported sodium hydrogen sulfate: As an efficient catalyst for the trimethyl, triethyl and t-butyl dimethyl silylations of aliphatic and aromatic alcohols in solution and under solvent-free conditions. *Journal of the Chinese Chemical Society*, 61(8), 929-934. <https://doi.org/10.1002/jccs.201300586>
- [12] Yao, H., Wang, Y., Razi, M. K. (2021). An asymmetric Salamo-based Zn complex supported on Fe₃O₄ MNPs: A novel heterogeneous nanocatalyst for the silyl protection and deprotection of alcohols under mild conditions. *RSC Advances*, 11(21), 12614-12625. <https://doi.org/10.1039/D1RA01185E>
- [13] Lu, A. -H., Salabas, E. L., & Schüth, F. (2007). Magnetic nanoparticles: Synthesis, protection, functionalization, and application. *Angewandte Chemie - International Edition in English*, 46(8), 1222-1244. <https://doi.org/10.1002/anie.200602866>
- [14] Majidi, S., Zeinali Sehriq, F., Farkhani, S. M., Soleymani Goloujeh, M., & Akbarzadeh, A. (2016). Current methods for synthesis of magnetic nanoparticles. *Artificial Cells, Nanomedicine, and Biotechnology*, 44(2), 722-734. <https://doi.org/10.3109/21691401.2014.982802>
- [15] Mohammadi, H., Nekobahr, E., Akhtari, J., Saeedi, M., Akbari, J., & Fathi, F. (2021). Synthesis and characterization of magnetite nanoparticles by co-precipitation method coated with biocompatible compounds and evaluation of *in-vitro* cytotoxicity. *Toxicology Reports*, 8, 331-336. <https://doi.org/10.1016/j.toxrep.2021.01.012>
- [16] Nayeem, J., Al-Bari, M. A. A., Mahiuddin, M., Abdur Rahman, M., Mefford, O. T., Ahmad, H., & Mahbubor Rahman, M. (2021). Silica coating of iron oxide magnetic nanoparticles by reverse microemulsion method and their functionalization with cationic polymer *P(NIPAm-co-AMPTMA)* for antibacterial vancomycin immobilization. *Colloids and Surfaces A : Physicochemical and Engineering Aspects*, 611, 125857. <https://doi.org/10.1016/j.colsurfa.2020.125857>
- [17] Unni, M., Uhl, A. M., Savliwala, S., Savitzky, B. H., Dhavalikar, R., Garraud, N., Arnold, D. P., Kourkoutis, L. F., Andrew, J. S., & Rinaldi, C. (2017). Thermal decomposition synthesis of iron oxide nanoparticles with diminished magnetic dead layer by controlled addition of oxygen. *ACS Nano*, 11(2), 2284-2303. <https://doi.org/10.1021/acs.nano.7b00609>
- [18] Maleki, S. T., Babamoradi, M., Rouhi, M., Maleki, A., & Hajizadeh, Z. (2022). Facile hydrothermal synthesis and microwave absorption of halloysite/polypyrrole/Fe₃O₄. *Synthetic Metals*, 290, 117142. <https://doi.org/10.1016/j.synthmet.2022.117142>
- [19] Ramadan, I., Moustafa, M. M., & Nassar, M. Y. (2022). Facile controllable synthesis of magnetite nanoparticles via a co-precipitation approach. *Egyptian Journal of Chemistry*, 65(9), 59-65. <https://doi.org/10.21608/EJCHEM.2022.116869.5284>
- [20] Lyon, J. L., Fleming, D. A., Stone, M. B., Schiffer, P., & Williams, M. E. (2004). Synthesis of Fe oxide core/Au shell nanoparticles by iterative hydroxylamine seeding. *Nano Letters*, 4(4) 719-723. <https://doi.org/10.1021/nl035253f>
- [21] Zhang, M., Cushing, B. L., & O'Connor, C. J. (2008). Synthesis and characterization of monodisperse ultra-thin silica-coated magnetic nanoparticles. *Nanotechnology*, 19(8), 85601. <https://doi.org/10.1088/0957-4484/19/8/085601>
- [22] Perrotti, T. C., Freitas, N. S., Alzamora, M., Sanchez, D. R., & Carvalho, N. M. F. (2019). Green iron nanoparticles supported on amino-functionalized silica for removal of the dye methyl orange. *Journal of Environmental Chemical Engineering*, 7(4), 103237. <https://doi.org/10.1016/j.jece.2019.103237>
- [23] Li, H., Chen, X., Shen, D., Wu, F., Pleixats, R., & Pan, J. (2021). Functionalized silica nanoparticles: Classification, synthetic approaches and recent advances in adsorption applications. *Nanoscale*, 13(38), 15998-16016. <https://doi.org/10.1039/D1NR04048K>
- [24] Wang, C., Yang, L., Yuan, X., Zhou, W., Xu, M., & Yang, W. (2021). Fabrication of Ag nanoparticles supported on amino-functionalized peeled-watermelon structured silica-coated nano-Fe₃O₄ with enhanced catalytic activity for reduction of 4-nitrophenol. *Colloid and Interface Science Communications*, 45, 100521. <https://doi.org/10.1016/j.colcom.2021.100521>
- [25] He, H., Meng, X., Yue, Q., Yin, W., Gao, Y., Fang, P., & Shen, L. (2021). Thiol-ene click chemistry synthesis of a novel magnetic mesoporous silica/chitosan composite for selective Hg (II) capture and high catalytic activity of spent Hg (II) adsorbent. *Chemical Engineering Journal*, 405, 126743. <https://doi.org/10.1016/j.cej.2020.126743>

- [26] Park, M. E., & Chang, J. H. (2007). High throughput human DNA purification with aminosilanes tailored silica-coated magnetic nanoparticles. *Materials Science and Engineering: C*, 27(5-8), 1232-1235. <https://doi.org/10.1016/j.msec.2006.09.008>
- [27] Nayl, A. A., Abd-Elhamid, A. I., Aly, A. A., & Bräse, S. (2022). Recent progress in the applications of silica-based nanoparticles. *RSC Advances*, 12(22), 13706-13726. <https://doi.org/10.1039/D2RA01587K>
- [28] Bauer, I., & Knölker, H. -J. (2015). Iron catalysis in organic synthesis. *Chemical Reviews*, 115(9), 3170-1387. <https://doi.org/10.1021/cr500425u>
- [29] Li, S., Li, H., Tung, C. -H., & Liu, L. (2022). Practical and selective bio-inspired iron-catalyzed oxidation of Si-H bonds to diversely functionalized organosilanols. *ACS Catalysis*, 12(15), 9143-9152. <https://doi.org/10.1021/acscatal.2c02678>
- [30] Hu, P., Tan, M., Cheng, L., Zhao, H., Feng, R., Gu, W. -J. & Han, W. (2019). Bio-inspired iron-catalyzed oxidation of alkylarenes enables late-stage oxidation of complex methylarenes to arylaldehydes. *Nature Communications*, 10(1), 2425. <https://doi.org/10.1038/s41467-019-10414-7>
- [31] Farrar-Tobar, R. A., Wozniak, B., Savini, A., Hinze, S., Tin, S., & de Vries, J. G. (2019). Base-free iron catalyzed transfer hydrogenation of esters using EtOH as hydrogen source. *Angewandte Chemie - International Edition in English*, 58(4), 1129-1133. <https://doi.org/10.1002/anie.201810605>
- [32] Lu, P., Ren, X., Xu, H., Lu, D., Sun, Y., & Lu, Z. (2021). Iron-catalyzed highly enantioselective hydrogenation of alkenes. *Journal of the American Chemical Society*, 143(32), 12433-12438. <https://doi.org/10.1021/jacs.1c04773>
- [33] Kang, Y. C., Treacy, S. M., & Rovis, T. (2021). Iron-catalyzed photoinduced LMCT: A 1° C-H abstraction enables skeletal rearrangements and C(sp³)-H alkylation. *ACS Catalysis*, 11(12), 7442-7449. <https://doi.org/10.1021/acscatal.1c02285>
- [34] Roy, S., Das, S. K., Khatua, H., Das, S., Singh, K. N., & Chattopadhyay, B. (2021). Iron-catalyzed radical activation mechanism for denitrogenative rearrangement over C(sp³)-H amination. *Angewandte Chemie - International Edition in English*, 60(16), 8772-8780. <https://doi.org/10.1002/anie.202014950>
- [35] Radhika, S., Aneeraja, T., Philip, R. M., & Anilkumar, G. (2021). Recent advances and trends in the biomimetic iron-catalyzed asymmetric epoxidation. *Applied Organometallic Chemistry*, 35(6), e6217. <https://doi.org/10.1002/aoc.6217>
- [36] Mao, S., Budweg, S., Spannenberg, A., Wen, X., Yang, Y., Li, Y. -W., Junge, K., & Beller, M. (2022). Iron-catalyzed epoxidation of linear α -olefins with hydrogen peroxide. *ChemCatChem*, 14(4), e202101668. <https://doi.org/10.1002/cctc.202101668>
- [37] Gao, M., Li, W., Dong, J., Zhang, Z., & Yang, B. (2011). Synthesis and characterization of superparamagnetic Fe₃O₄@ SiO₂ core-shell composite nanoparticles. *World Journal of Condensed Matter Physics*, 1(2), 49-54. <https://doi.org/10.4236/wjcmp.2011.12008>
- [38] Sheykhan, M., Yahyazadeh, A., & Ramezani, L. (2017). A novel cooperative Lewis acid/Bronsted base catalyst Fe₃O₄@SiO₂-APTMS-Fe(OH)₂: An efficient catalyst for the Biginelli reaction. *Molecular Catalysis*, 435, 166-173. <https://doi.org/10.1016/j.mcat.2017.03.032>
- [39] Sanati, A. M., Kamari, S., & Ghorbani, F. (2019). Application of response surface methodology for optimization of cadmium adsorption from aqueous solutions by Fe₃O₄@SiO₂@APTMS core-shell magnetic nanohybrid. *Surfaces and Interfaces*, 17, 100374. <https://doi.org/10.1016/j.surfin.2019.100374>
- [40] Gonzalez-Carrillo, G., Gonzalez, J., Emparan-Legaspi, M. J., Lino-Lopez, G. J., Aguayo-Villarreal, I. A., Ceballos-Magaña, S. G., Martinez-Martinez, F. J., & Muñoz-Valencia, R. (2020). Propylsulfonic acid grafted on mesoporous siliceous FDU-5 material: A high TOF catalyst for the synthesis of coumarins via Pechmann condensation. *Microporous and Mesoporous Materials*, 307, 110458. <https://doi.org/10.1016/j.micromeso.2020.110458>

Additional information

Correspondence and requests for materials should be addressed to S. Mehdigholami.

HOW TO CITE THIS ARTICLE

Mehdigholami, S.; Koohestanian, E. (2023). Fe₃O₄@SiO₂/AEPTMS/Fe(OTf)₃: An efficient superparamagnetic nanocatalyst for the protecting of alcohols. *J. Part. Sci. Technol.* 9(1) 1-9.

DOI: [10.22104/JPST.2023.6188.1224](https://doi.org/10.22104/JPST.2023.6188.1224)

URL: https://jpst.irost.ir/article_1276.html